Journal of Organometallic Chemistry 880 (2019) 322–332

Contents lists available at ScienceDirect

Journal of Organometallic Chemistry

journal homepage: www.elsevier.com/locate/jorganchem

Polymer immobilized [Mg@PS-anthra] complex: An efficient recyclable heterogeneous catalyst for the incorporation of carbon dioxide into oxiranes at atmospheric pressure and Knoevenagel condensation reaction under solvent free condition

Ranjan Kumar Mondal [a], Sk Riyajuddin [b], Aniruddha Ghosh [a, 1], Swarbhanu Ghosh [a, 1], Kaushik Ghosh [b, **], Sk.Manirul Islam [a, *]

[a] Department of Chemistry, University of Kalyani, Kalyani, Nadia, 741235, W.B, India
[b] Institute of Nano Science and Technology, Mohali, Punjab, 160062, India

ARTICLE INFO

Article history:
Received 9 October 2018
Received in revised form
5 November 2018
Accepted 16 November 2018
Available online 20 November 2018

Keywords:
Heterogeneous catalyst
Mg@PS-anthra complex
Cyclic carbonate
CO_2 fixation
Knoevenagel condensation

ABSTRACT

Chemical fixation of CO_2 into the organic molecules is very challenging from the perspective of greenhouse gas consumption and manufacturing of chemicals with C1 backbone. The process was developed with the synthesis of an efficient polystyrene functionalized Magnesium-anthranilic acid complex (Mg@PS-anthra). The catalytic system was successfully explored as a heterogeneous catalyst for the synthesis of cyclic carbonates by CO_2 fixation at atmospheric pressure and Knoevenagel condensation reaction under room temperature solvent free condition. The material was thoroughly characterized by diffuse reflectance UV-vis, FTIR spectroscopy, thermal gravimetric analysis (TGA), scanning electron microscopy (SEM), energy-dispersive X-ray spectroscopy (EDX) and powder X-ray diffraction (PXRD) techniques. The catalytic pathway has been investigated for the cyclo-addition reaction of epoxides using atmospheric CO_2 accompanied by the Knoevenagel condensation reaction with a variety of different aldehydes over cost effective environmental friendly Mg-catalyst. This is attributed to its high catalytic activity, recovery simplicity and excellent five times recycling efficiency; without any substantial decrease in catalytic performance.

1. Introduction

Carbon dioxide is one of the primary components of greenhouse gas emerging out through various human and continuous industrial activities running in the environment. Accumulation of CO_2 is a very challenging aspect to the modern chemist for recompensing the utilization of abundant CO_2 in nature eventually. The excess concentration of carbon dioxide in the atmospheric layers over the last few decades of human civilization is an obsessing problem in our society [1]. The source of energy is fossil fuels upon burning leads to carbon dioxide, which has the high capacity to heat storage that leads to the warming of atmosphere [2]. Carbon capture and separation (CCS) has recently been proved as the most fascinating technique for regulating the unremitting release of greenhouse gases. Though, CCS meets several operational and commercial limitations to develop on a large scale. One of the vital economic drawbacks is that it is not a cost-effective movement that requires large capital investment. Later, a carbon capture and utilization (CCU) process has been introduced to draw attention since it can transform emitting CO_2 gas from power plants into valuable products such as chemicals and fuels. The power station flue gas contains the very small extent of CO_2 than pure CO_2 and is contaminated by numerous impurities and solid particulate matter. Several functional and metal based catalysts have been designed for CO_2 capturing and its exclusive separation with high CO_2 recovery rate in a power plant flue gas for the catalytic transformations. This area of current discussion will convey the scenario for upcoming research on further practical based CO_2 capture and separation for conversion into cyclic carbonates directly from power plant flue gas [2,3]. Therefore, the advancement of an efficient catalytic process

* Corresponding author.
** Corresponding author.
E-mail addresses: kaushik@inst.ac.in (K. Ghosh), manir65@rediffmail.com (Sk.Manirul Islam).
[1] These authors contributed equally.

https://doi.org/10.1016/j.jorganchem.2018.11.026
0022-328X/

for CO_2 transformations into useful chemical compounds has become an unveiling issue in the arena of benign and sustainable synthetic procedures [3,4]. Out of the several demanding and economic CO_2 transformations of utilizing C1 backbone is established to date, the most industrially efficacious process is a cycloaddition reaction between CO_2 and epoxide [5].

The generation of cyclic carbonates have been accomplished through fixation of CO_2 on epoxide over a wide range of homogeneous and heterogeneous catalysts such as crown ether [6], mixed oxides [7], ionic liquids [8], alkali metal salts [9], Schiff-base or metal complexes [10], organic bases [11], quaternary ammonium or phosphonium salts [12], functionalized MOFs [13], zeolite [14] and titanosilicates [15].

The major concern for the chemical fixation of CO_2 is the low energy level of the CO_2 molecule itself which requires stringent conditions such as air sensitivity, high temperature and high pressure. Hence, it is a very challenging task to furnish an effective catalyst embedded with suitable polymer moiety for the synthesis of fine chemicals through CO_2 fixation process in the context of green chemistry. The five or six membered cyclic carbonates are tremendous aprotic solvents of polar nature. The synthesized organic cyclic carbonates have broadly appeared as intermediates for the production of pharmaceuticals, carbamates, biomedical agents, engineering materials and can be applied as electrolyte components in Li-ion batteries [16,17].

Apart from CO_2 transformations in organic synthesis, the carbon–carbon bond formation reactions have also significant industrial applications in high added value chemicals synthesis. One such significant and largely useful C–C bond forming reaction is Knoevenagel condensation between aldehydes and active methylene moieties. The reactions are frequently catalyzed by bases [18] such as ammonia, Graphene based material, amines, or sodium ethoxide in organic solvents. Ionic liquids [19], lewis acids [20], surfactants [21] and zeolites [22] have also been applied to catalyze this reaction. In practise the environmental friendly solvents like water in association with solvent-free reactions are expressively convenient in terms of economical, benign and green chemical procedures [23]. The advantage of using water or other green solvents not only eliminate the toxicity of organic solvents but also enhance the reaction rate in organic synthesis. A variety of homogeneous catalysts are exploited for cyclo-addition of epoxides via CO_2 fixation and Knoevenagel condensation reactions over several years [24]. Now the fact is there are certain difficulties in homogeneous catalysts such as the catalysts are destroyed, and cannot be isolated or reused further. From this perspective, the development of unique heterogeneous base catalysts has gained extensive attention and is successfully applied throughout the synthesis to eliminate the above limitations.

Therefore it is very necessary to design an efficient, low cost, eco-friendly, and highly selective heterogeneous solid catalyst to attain the desired selective product. The heterogeneous catalysts have been used for numerous organic transformations on account of easy recovery and recycle of the catalyst from reaction mixture [25].

Regarding this research work, generally alkaline earth metal oxides like CaO, BaO and MgO are commonly used as the active site enables to functioning as solid basic catalysts. Particularly, MgO can potentially increase the catalytic activity due to their enormous basic features [26–30]. Hence, it may be expected that a combined material prepared by the Mg species coordinated with Merrifield resin (PS) tagged anthranilic acid ligand could play efficient catalytic performance in the Knoevenagel condensation reaction. This could be assigned to the distinctive chemical structure of Mg@PS-anthra complex along with the tremendous basicity of the Mg species.

Cinnamic acid with its corresponding esters is extensively synthesized by Knoevenagel condensation reactions. Very essential components such as perfumes, flavours, synthetic indigo and pharmaceuticals are prepared from the carboxylic functional derivatives of cinnamic acid [31,32].

In this work, we have simply demonstrated the preparation of efficacious heterogeneous base catalyst namely Mg@PS-anthra complex by the reaction of Merrifield resin tagged with anthranilic acid and Mg metal. Catalytic investigations on Mg@PS-anthra complex have been accomplished for the cycloaddition reaction between different epoxides and carbon dioxide at atmospheric pressure. Additionally, the catalyst was proved magnificent in the Knoevenagel Condensation reaction using several aldehyde derivatives under solvent free condition at room temperature. The recycling performance and the catalytic efficiency of Mg@PS-anthra complex material were examined for the cycloaddition of oxirane along with the Knoevenagel condensation reaction.

2. Experimental section

2.1. Materials

All chemicals and reagents were A.R. grade. Chloromethylated polystyrene was received from Sigma-Aldrich Company (USA) and other chemicals were available from Alfa aesar (India). Magnesium(II) chloride was purchased from Merck (India). The reagents were used as received without further purification. Reagent grade solvents were distilled and dried according to the standard methods before use.

2.2. Characterization techniques

A Perkin Elmer, 2400C, USA elemental analyzer was operated to collect the microanalytical data (C, H and N). The amount of metal content was determined by Optima 2100DV instrument (ICP-AES, Perkin Elmer). Scanning electron microscopy (SEM) measurements of the synthesized materials were ensured with the help of a JEOL JEM 6700F field-emission scanning electron microscope. Powder X-ray diffraction (PXRD) patterns of the Mg@PS-anthra material was recorded through a Bruker D8 Advance X-ray diffractometer using the Ni-filtered Cu Kα ($\lambda = 0.15406$ nm) radiation. FT-IR spectra of the samples were monitored using KBr pellets in a Perkin-Elmer FT-IR 783 spectrophotometer instrument. The Shimadzu UV-2401 PC doubled beam spectrophotometer connected to an integrating sphere attachment was successively utilized in order to observe the UV-Vis spectra of the solid samples with a certain time. Mettler-Toledo TGA-DTA 851e instrument provided the thermogravimetric analysis (TGA) of the material. The Atomic absorption spectrophotometer (Model Varian AA240) was utilized to estimate the % content of magnesium in the Mg@PS-anthra catalyst quantitatively. The Varian 3400 gas chromatograph equipped with a 30 m CP-SIL 8CB capillary column and a flame ionization detector precisely analyzed the reaction products obtained after completion of the reactions. The products were identified by comparing with the corresponding authentic samples.

2.3. Preparation of Mg@PS -anthra complex catalyst

The Mg@PS-anthra complex was prepared according to the method described in the earlier literature [33]. At the beginning, the Merrifield resin (1) (500 mg) was added to react with anthranilic acid (250 mg) dissolved in DMF (5 mL) under the reflux condition for 30 h to yield the polymer supported ligand (2). This polymer supported ligand (1 g) then reacted with $MgCl_2.6\ H_2O$ (0.1 g) in ethanol (10 mL) for 9 h at 70 °C to produce the resultant

polymer grafted Mg catalyst (3). The outline for the preparation of polymer supported metal complex catalyst is given below (Scheme 1):

The ICP-AES spectroscopy provided the elemental analysis for the synthesized Mg@PS-anthra complex containing the Mg loading close to 4.26% by weight (Table 1). The elemental analysis provided 3.78 wt% of Cl in the Mg@PS-anthra complex. The calculated molar ratio of Cl/Mg 1.1 is in line with the suggested structure (3) [(PS-anthra)MgCl]. Additionally, the presence of 1.16 wt% of N corresponding to a molar ratio of N to Mg ~1.1 was computed by the data acquired from elemental analysis. The value of N/Mg = 1 is within the range of uncertainty in the elemental analysis (±10%) and is almost identical with expected structure (3). The above analysis substantially indicates the presence of 2.45 wt% Cl (i.e elimination of 1.33 wt% Cl in ligand from 3.78 wt% Cl in the complex) in Mg@PS-anthra complex (Table 1). This 2.45 wt% of Cl in Mg@PS-anthra complex comes exclusively from $MgCl_2.6H_2O$. The obtained data for structure (3) was supportive to analyze the determination of molar Cl/Mg ratio close to 1.1 [34,35].

2.4. Typical procedure for synthesis of cyclic carbonates at 1 atmospheric pressure of CO_2

The reaction was executed by using epoxide (5 mmol), TBAB (Bu_4NBr) (5 mol %), and Mg@PS-anthra complex (30 mg) into a 100 ml of round bottom flask fitted with magnetic stirring bar. After mixing the reactants one after the other in the round bottom flask, it was followed by fitting with a CO_2 balloon under the appliance of 1 atm pressure. The reaction mixture was stirred at room temperature for 3–6 h. After completion of the reaction, the polymer supported catalyst was filtered and the crude product was removed then dried in an oven. The filtrate was extracted up to five times with ethyl acetate and washed several times with water. The column chromatography was carried out with the isolated five-membered organic carbonates.

2.5. General procedure for Knoevenagel condensation reaction

The heterogeneous catalyst Mg@PS-anthra was stirred with 2 mmol of ethyl cyanoacetate in 50 ml round bottle flask for 45 min at room temperature. The respective aldehyde (1 mmol) was added to this mixture and the resulting mixture was stirred for the appropriate time at room temperature. After the end of the reaction, the reaction mixture was treated with dichloromethane followed by successive separation of organic and aqueous layers by using separating funnel. Na_2SO_4 was added to the organic layer to remove the aqueous content. All the yields of individual esters were calculated from the isolated product.

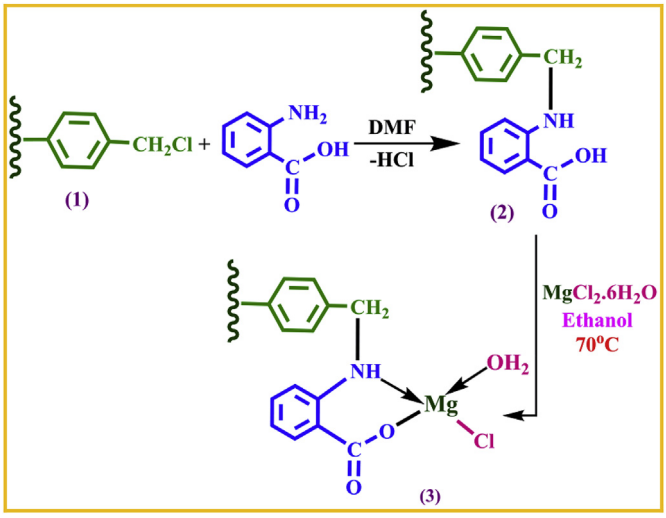

Scheme 1. Schematic representation of the synthesis of polymer supported Mg@PS-anthra complex.

3. Results and discussion

3.1. Characterization of Mg@PS-anthra complex

3.1.1. Powder X-ray diffraction analysis

The Mg@PS-anthra complex exhibits a broadband at the range of 2θ (10–30) clearly suggesting the amorphous nature of the catalyst [36]. Consequently, there was no indication of any nanocrystalline nature of the MgO material detected in the synthesized Mg@PS-anthra complex during the introduction of Mg-metal into the ligand (Fig. 1).

3.1.2. Microscopic analysis

Scanning electron micrographs (SEM) support to ascertain the morphological changes between polymer-supported ligand and the Mg@PS-anthra complex on the polymer matrix. The SEM images of the polymer-supported ligand (a) and the Mg@PS-anthra complex (b) are described in Fig. 2. SEM images provided a qualitative approach about the alteration in morphology between PS-anthra ligand and the Mg@PS-anthra complex (Fig. 2b). It was clearly observed the Mg@PS-anthra complex that quite roughening of the ligand attached polystyrene surface appeared when coordinated to magnesium metal. In addition, the EDX data also facilitates to determine the attachment of metal on the polymer surface (Fig. 3). There observed no remarkable changes in morphology pattern between the synthesized Mg@PS-anthra complex and the reused Mg@PS-anthra catalyst.

3.1.3. UV-visible spectra

Another evidence for the presence of Mg supported on polymer material was attained with the help of UV-vis spectra. The polymer attached Mg catalyst has some limitations of its solubility in known organic solvents. As a consequence, the UV-vis spectra of the catalyst has been achieved in reflectance diffused spectrum mode using $BaSO_4$ as a reference. The UV-vis reflectance diffused spectra of the produced PS-anthra ligand and the Mg@PS-anthra complex has been indicated in Fig. 4. The UV-vis absorption spectrum of the Mg@PS-anthra complex was revealed near 255 nm wavelength. The respective absorption bands at 232, 255 and 344 nm for the pure ligand are assigning the characteristic π-π* electronic transitions responsible for the aromatic ring. When PS-anthra ligand was coordinated to Mg, a new band observed at 350 nm. It may be due to the charge transfer transitions between coordinated atoms of the ligand and the central Mg atom [37].

3.1.4. Thermogravimetric analysis

The PS-anthra ligand and Mg@PS-anthra complex were taken in an air atmosphere at a heating rate of 10 °C min^{-1} to study the thermogravimetric analysis (TGA). As realized from Fig. 5 the synthesized Mg@PS-anthra complex is reasonably stable up to 470 °C, however, PS-anthra ligand decomposes at slight lower temperature 420 °C. The thermal stability of Mg@PS-anthra catalyst is sufficiently improved as a result of the coordination followed by complexation with magnesium metal. The corresponding studies of DTA support that the stages of decomposition are exothermic in nature (not shown).

Table 1
Chemical composition polymer-anchored ligand and its Mg catalyst.

Compound	Colour	C (%)	H (%)	N (%)	Cl (%)	Mg loading (%)
PS-anthra ligand	Pale yellow	83.98	7.94	4.23	1.33	-
Mg@PS-anthra complex	Pale yellow	79.44	7.39	1.16	3.78	4.26

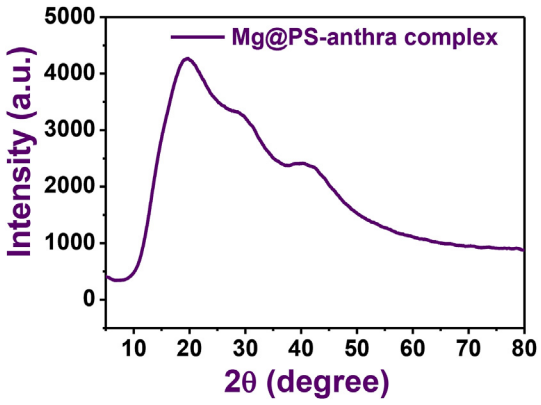

Fig. 1. PXRD of Mg@PS-anthra complex.

3.1.5. FT IR spectra

The binding mode of anthranilic acid and magnesium metal onto the Merrifield resin has been established by infrared spectral data in 4000-400 cm^{-1} regions. The FT-IR spectrum of the PS-anthra ligand shows a very weak band or absence of C—Cl peak (due to $-CH_2Cl$ groups) near 1264 cm^{-1}. The appearance of a strong band at 3382 cm^{-1} (ν-NH, the secondary amine) and disappearance of (ν-C—Cl) band upon reacting with anthranilic acid implies the formation of covalent bond through N atom. The other distinctive peaks at 1702 (ν C═O), 3449 (ν —OH), 3364 (ν-NH), 1403 (νsym COO) and 1552 cm^{-1} (νasym COO) confirmed also the formation of PS-anthra ligand [38]. When PS-anthra ligand coordinated to magnesium metal, the shifting of peaks towards the lower wave-number regions (1407 for νsym- COO, 1562 for νasym —COO and 3282 for ν N—H respectively) implies the participation of the $-NH_2$ and COOH functional groups of anthranilic acid in the development of the Mg@PS-anthra complex (Fig. 6).

3.2. Catalytic activity

3.2.1. Synthesis of cyclic carbonates catalyzed by polymer supported Mg@PS-anthra complex

CO_2 insertion on oxiranes initiates the formation of a five membered organic cyclic carbonates by polymer supported Mg-based catalyst in presence of TBAB (Bu_4NBr) (Scheme 2).

Application of CO_2 fixation and/or conversion is potentially important for the fruitful utilization of abundant greenhouse CO_2 gas into value added chemicals. In order to optimize the yield of the five-membered cyclic carbonates, we have tested all the reaction parameters such as time, amount of Bu_4NBr (co-catalyst). The production of styrene carbonate from the cyclo-addition reaction of CO_2 with styrene oxide is selected as the model example for this reaction (Table 2). From Table 2 it is clear that among the different amount of Bu_4NBr used, 5 mol% exhibited the best conversion (entry 10). Further, we have also checked the influence of reaction time on the yield of the products (Table 2, entries 1–10). The best output was achieved when carrying out the reaction with 5 mol% of Bu_4NBr in presence of 30 mg of the catalyst at 1 atmospheric pressure and RT for 6 h.

Reactions experienced with smaller and higher than the actual reaction completion time consequences to the incomplete styrene oxide conversions and relatively lower yield of the product (Table 2, entry 1–3). For the lower amount of Bu_4NBr, the reaction did not proceed completely and hence resulting in a lower yield of the product (Table 2, entries 4 and 5). In presence of Bu_4NBr alone without catalyst and in absence of Bu_4NBr with catalyst, it was observed that trace amount of products were obtained in the same conditions (Table 2, entry no. 8 and 9).

In order to scrutinize the optimization reaction conditions, we have thoroughly examined the activities of Mg@PS-anthra complex for the generation of cyclic carbonate through CO_2 fixation reaction. A long range of oxiranes such as styrene oxide, allyl glycidyl ether,

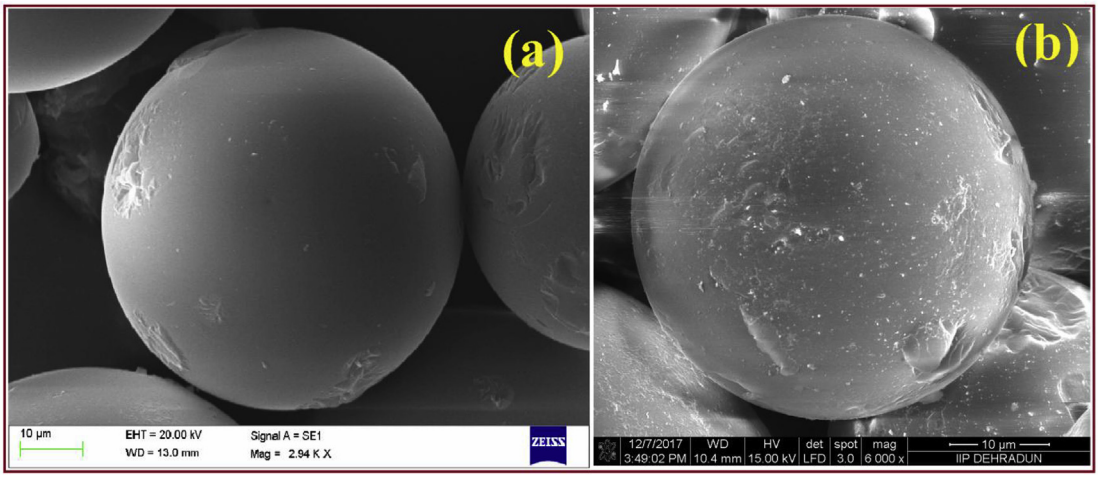

Fig. 2. FE-SEM picture of PS-anthra ligand (a) and Mg@PS-anthra complex (b) respectively.

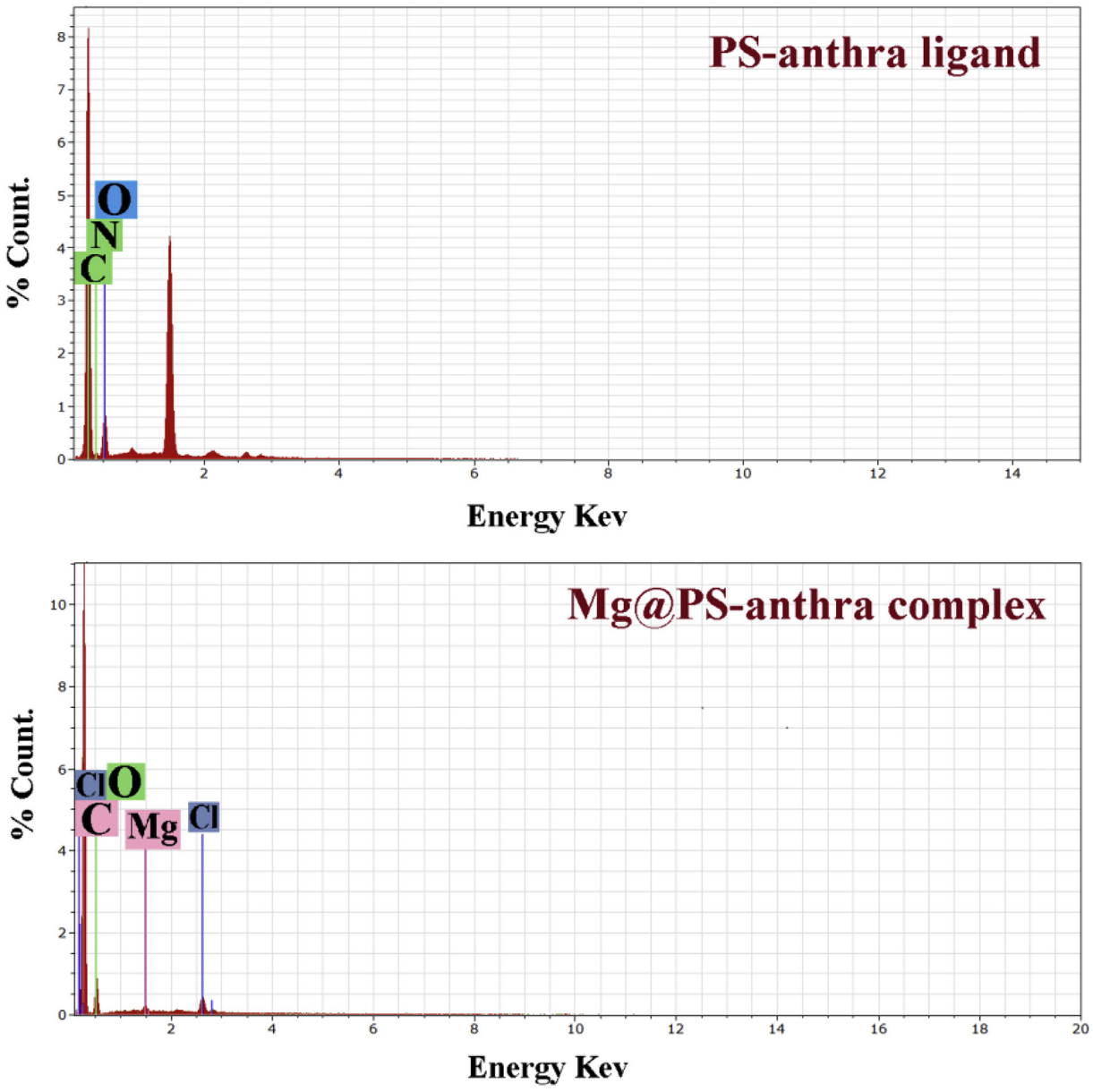

Fig. 3. EDX spectra of PS-anthra ligand and Mg@PS-anthra complex.

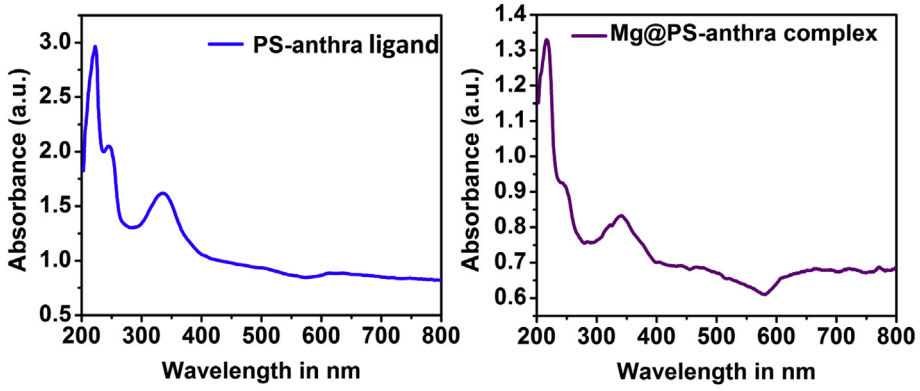

Fig. 4. The UV-visible absorption spectrum of PS-anthra ligand and Mg@PS-anthra complex.

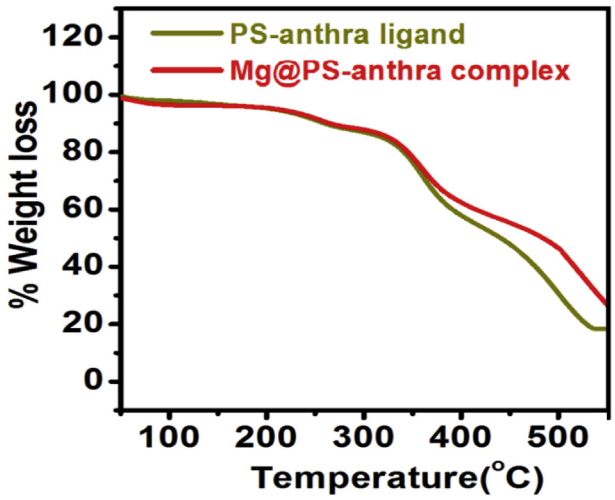

Fig. 5. Thermogravimetric analyses of PS-anthra ligand and Mg@PS-anthra complex.

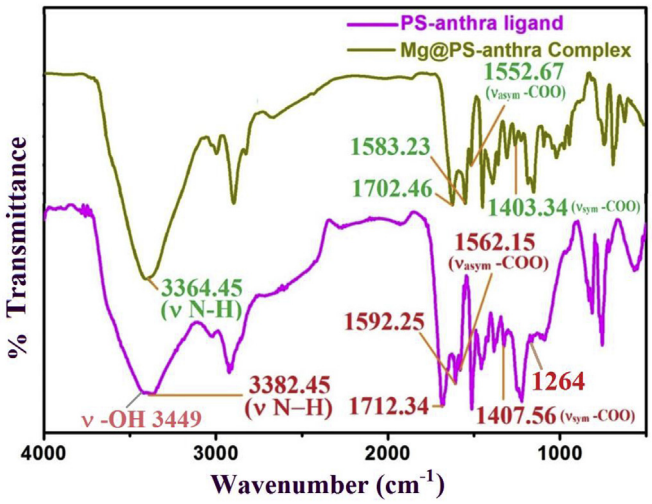

Fig. 6. FT IR spectra of PS-anthra ligand and Mg@PS-anthra complex.

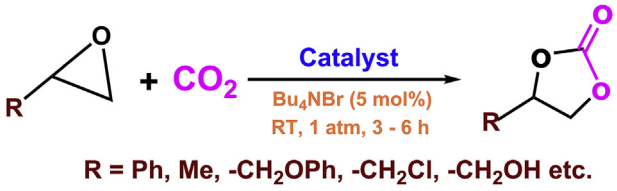

Scheme 2. Preparation of organic cyclic carbonates from CO_2 and epoxides.

propylene oxide, epichlorohydrin, aryloxy epoxides (1, 2-epoxy-3-phenoxy propane) and glycidol (epoxides with substituted functional groups) have been used as substrates. The experimental results are summarized in Table 3. Most of the oxiranes could be easily converted to organic five-membered cyclic carbonate derivatives via CO_2 fixation with reasonable selectivity and high yield. It is worth mentioning that the electron-releasing (Table 3, entries 1–3) and electron-withdrawing groups (Table 3, entry 4) attached on the terminal epoxides has no effect on the yield of the products. Additionally, we have performed our experiments using aromatic oxirane derivatives like 2-(4-fluorophenyl) oxirane and 2-(4-chlorophenyl) oxirane (Table 3, entry 7,8). The results of this

Table 2
Optimization of reaction conditions for the synthesis of styrene carbonate.[a]

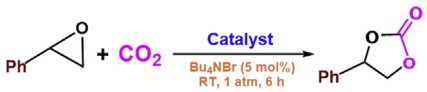

Entry	Bu_4NBr (mol %)	Time (h)	CO_2 pressure (atm)	Yield[b] (%)
1	5	1	1	45
2	5	2	1	54
3	5	3	1	60
4	3	3	1	52
5	4	3	1	64
6	5	4	1	75
7	5	5	1	82
8[c]	5	6	1	Trace
9	0	6	1	Trace
10	5	6	1	97

[a] Reaction conditions: Styrene oxide (5 mmol), catalyst (30 mg), RT.
[b] GC yield of cyclic carbonate.
[c] Without catalyst.

substituted aromatic oxiranes in this cyclic carbonate synthesis show that there is no noticeable change in yield percentage of product compared to the other substrates. Due to the low boiling point (34 °C) of the substrate propylene oxide, it offered comparatively lower yields (Table 3, entry 1).

The time of reaction has been varied under optimized reaction conditions to explore the complete potential of Mg@PS-anthra catalyst in the cycloaddition reaction until the full conversion of SO is completed. The summary for the reaction time with conversion and selectivity has been represented in Fig. 7. From the graph, it is found that the conversion of styrene oxide linearly increases over time from the initial to 6 h and then in the remaining 2 h it retained the 97% conversion level, whereas the selectivity of styrene carbonate remained nearly 100% during the entire period of reaction. From Fig. 7 it is evident that 6 h reaction time is sufficient to complete this CO_2 fixation reaction at room temperature.

The quantity of catalyst has a significant role in this reaction (Fig. 8). When the catalyst amount was used in 10 mg and 20 mg during the reaction the conversions were 30% and 60% respectively. It was noticed that optimum conversion was observed when 30 mg of catalyst was used. Nevertheless, no further increase in the product yield with a further rise in the catalyst amount exceeding 30 mg.

3.2.2. Possible mechanistic pathway for the synthesis of cyclic carbonates

In the first step, the CO_2 molecule is efficiently activated by the Mg@PS-anthra complex to afford a three membered Mg-active intermediate [39] (Scheme 3). The Mg centre presents in the Mg@PS-anthra catalyst surface can act as facile electron donors [40] for the activation of the CO_2 molecules. The subsequent step is the attack of substrate oxirane through the coordination of O atom and Mg centre of the polymer attached catalyst followed by ring opening of epoxide. The produced Mg-coordinated epoxide intermediate is initiated by the nucleophilic attack through Br^- ion from quaternary salt on the less hindered side of epoxide, leads to an oxyanion species. The oxyanion generated from ring opening then attacks the carbon atom of the carbon dioxide molecule to produce another oxyanion Mg-species. At this stage Br^- group leaves the product by which the respective cyclic carbonate is formed, and it desorbed from the catalyst surface as soon as the Mg@PS-anthra catalyst gets back to its initial state [41]. The kinetic studies of the corresponding reactions have been executed by varying the

Table 3
Preparation of organic cyclic five-membered carbonates over Mg@PS-anthra catalyst under optimized conditions.

Entry	Epoxide	Product	Time (h)	Yield[a] (%)
1			6	86
2	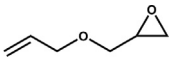	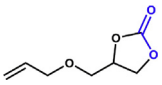	6	94
3	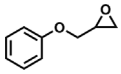	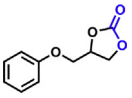	6	95
4		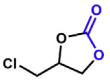	6	90
5	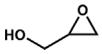	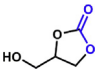	6	87
6		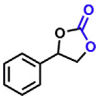	6	97
7	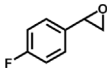	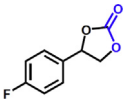	6	81
8	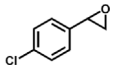	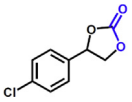	6	78

Reaction conditions: Styrene oxide (5 mmol), Catalyst (30 mg), Co-catalyst TBAB (5 mol %), CO_2 pressure (1 atm).
[a] Yield was determined by GC.

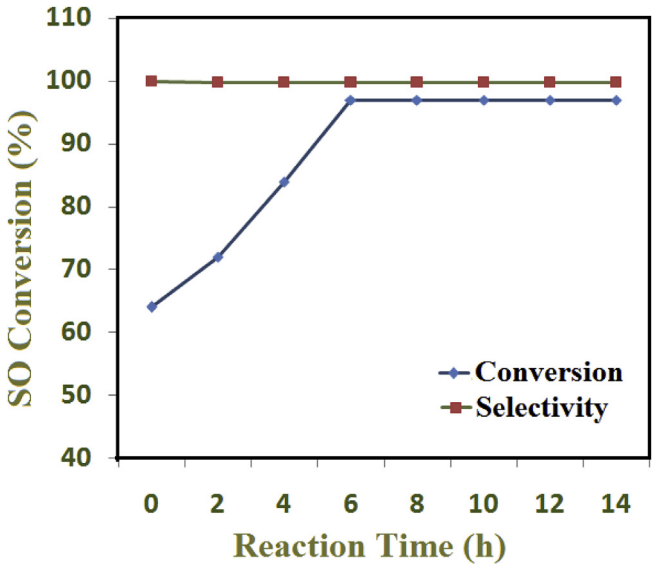

Fig. 7. Effect of reaction time on the conversion of SO to SC over Mg@PS-anthra complex.

concentration of epoxide and CO_2 pressure, keeping the other parameters unaltered. The reactions followed first-order reaction kinetics as monitored from the kinetics measurements. The rate of

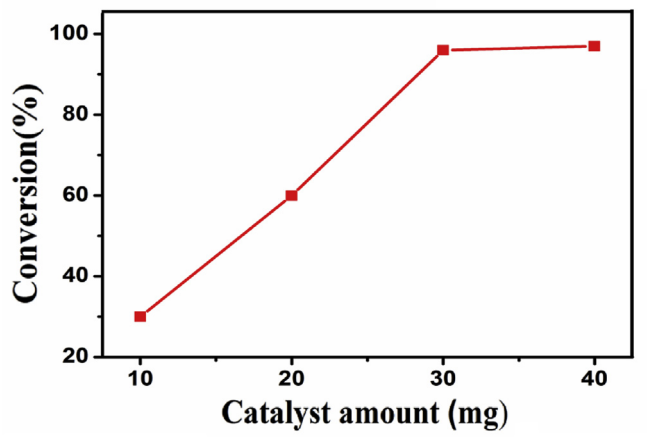

Fig. 8. Effect of the amount of catalyst for the CO_2 fixation over Mg@PS-anthra complex.

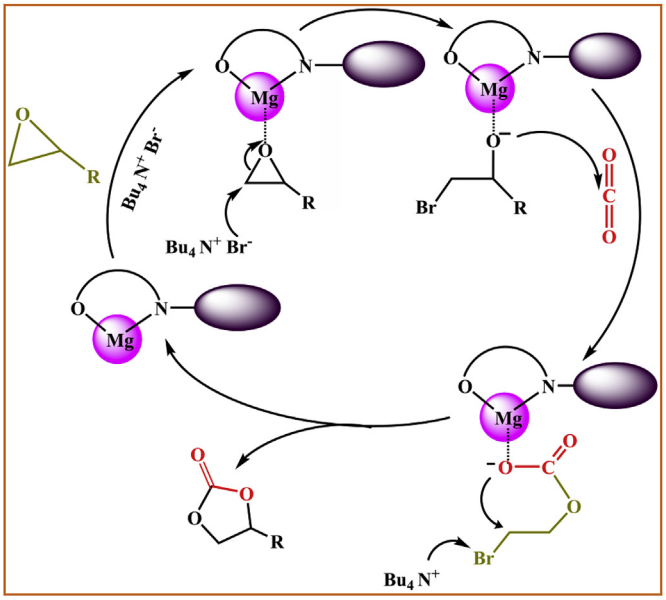

Scheme 3. Proposed mechanistic pathway for the synthesis of cyclic carbonates catalyzed by Mg@PS-anthra complex.

the cycloaddition of CO_2 on epichlorohydrin could be determined by altering the concentrations of catalyst, tetrabutylammonium bromide and CO_2 [42]. Hence the rate of this reaction can be written as: rate = k[epoxide]^1[CO_2]^1[[Mg@PS-anthra complex]^1[Bu_4NBr]^2.

3.3. Knoevenagel condensation reaction

The catalytic activity of the Mg@PS-anthra complex was scrutinized for the Knoevenagel condensations between benzaldehyde and ethyl cyanoacetate to prepare benzylidene ethyl cyanoacetate as the predominant product (Scheme 4).

Romero et. al. [43] reported the amine-functionalized SBA-15 catalyst contributing 98% conversion in the Knoevenagel condensation reaction at 105 °C. However, at room temperature amine-functionalized MCM-41 showed 81% conversion as reported by Sugi et al. [44]. The typical drawbacks came upon with these methods were either higher temperature or requirement of long reaction time to yield the corresponding products. However, in this present study, we have got fascinating results attributed to the

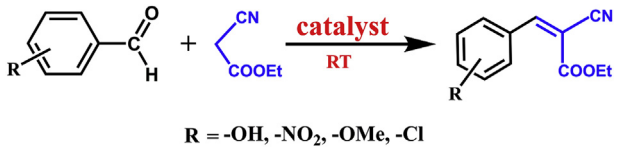

Scheme 4. Knoevenagel condensation reaction of benzaldehyde with ethyl-cyanoacetate using the Mg@PS-anthra catalyst.

presence of basic sites in the synthesized Mg@PS-anthra complex. According to the principles of green chemistry, we are highly motivated to perform the reaction under room temperature and solvent free conditions. Initially, we have monitored that no reaction found in the absence of Mg@PS-anthra complex, whereas Mg@PS-anthra complex effectively catalyzed the Knoevenagel condensation reactions leading to the high yield of benzylidene ethylcyanoacetate. This fact is accounted for the presence of basic sites in Mg@PS-anthra complex. After this experiment, we have examined the effects of various reaction parameters on the condensation between benzaldehyde with ethyl-cyanoacetate to produce benzylidene ethyl-cyanoacetate using Mg@PS-anthra as a catalyst. The molar ratio of benzaldehyde to ethyl-cyanoacetate for the condensation reaction is 1:4, 1:3, 1:2, and 1:1 respectively (Fig. 9). At a benzaldehyde to ethyl-cyanoacetate molar ratio of 1:2, the catalyst gives higher yield, 97% in 2 h. The selectivity towards the product benzylidene ethyl-cyanoacetate was 98%.

Further increasing the concentration of ethylcyanoacetate, the conversion remains almost the same but the selectivity got decreased. This is due to the rise in ethylcyanoacetate concentration in the reactant mixture; the self-condensation process may occur within the ethylcyanoacetate molecules.

Throughout the condensation reaction, the effect of reaction time on conversion and selectivity of the product under the Mg@PS-anthra catalyst are shown in Fig. 10. It has been noted that the conversion and selectivity are increasing up to 2 h. Later the reaction became slower and reached a maximum. The % of conversion and product selectivity values did not vary considerably with a further increase in reaction time.

The catalyst Mg@PS-anthra exhibits a reasonable activity in the Knoevenagel condensation reaction due to its structural basicity. We have executed several substituted aldehydes and active ethyl-cyanoacetate with the molar ratio of 1:2 to explore the

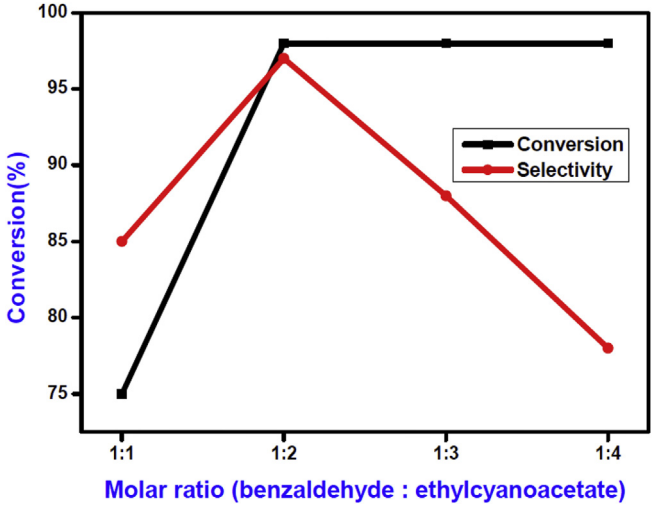

Fig. 9. The effect of molar ratios of benzaldehyde and ethylcyanoacetate towards Knoevenagel condensation reaction.

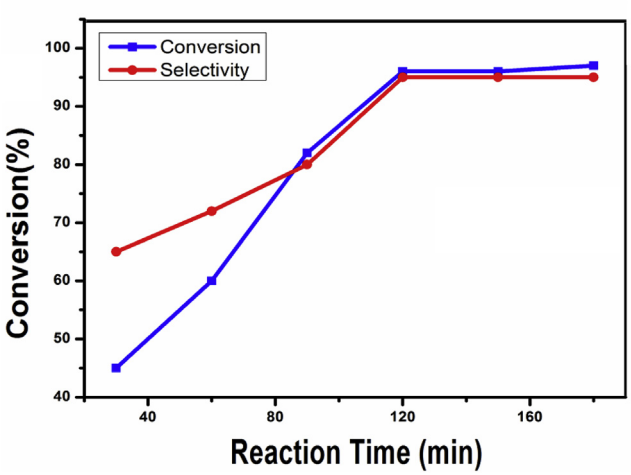

Fig. 10. Effect of reaction time on Knoevenagel condensation reaction.

functionality of Mg@PS-anthra in Knoevenagel condensation. In this reaction ethylcyanoacetate and the substituted benzaldehydes containing electron releasing groups *e.g.* $-CH_3$, decreased the conversion rate and yield of the product although the electron withdrawing substituents like $-NO_2$ on the aromatic ring significantly increased the conversion and contributed high product yield (Table 4). The scope of the reaction was elaborated using heterocyclic aldehydes *e.g.* furan-2-carbaldehyde and thiophene-2-carbaldehyde (Table 4, entry 9, 10). The data represented in Table 4 suggests that yield of the respective heterocyclic products is slightly lower than that of the aromatic aldehydes.

The plausible mechanism [45] for the Knoevenagel condensation reaction has been shown in Scheme 5. It is assumed that Mg centre facilitates the Knoevenagel type coupling by co-ordinating to oxygen atom of carbonyl groups. Initially, by the attack of the base catalyst Mg@PS-anthra complex, the ethylcyanoacetate molecule loses its acidic proton to form an anionic reactive enolate intermediate. In this process, the Mg centre of the Mg@PS-anthra can activate ethylcyanoacetate so that deprotonation occurs from the ethylcyanoacetate moiety. The next step is the nucleophilic attack of this anion at the electron deficient carbonyl centre of benzaldehyde. Simultaneous abstraction of the proton takes place from the protonated Mg@PS-anthra catalyst accordingly the production of the Mg-coordinated β-hydroxyl species together with the regenerated catalyst. The final desired products can be achieved via the dehydration of the β-hydroxyl intermediate.

3.4. Evaluation of catalytic activity of Mg@PS-anthra catalyst with the earlier reported systems

The evaluation of efficiency for the Mg@PS-anthra catalyst with the other reported catalyst for the present reactions is assigned in Table 5. The following comparison reveals that the polymer tagged Mg-catalyst is more worthy and well enough than the earlier catalyst. From the tally of the related former catalytic systems involving production of organic five-membered cyclic carbonates under 1 atm CO_2 pressure along with Knoevenagel condensation products, it has appeared that our Mg@PS-anthra complex executed greater efficiency under ambient conditions.

3.5. Recyclability of Mg@PS-anthra complex catalyst

After completion of the reaction, the Mg@PS-anthra catalyst was separated out from the final reaction mixture by applying gentle

Table 4
Knoevenagel condensation of different aldehydes with ethylcyanoacetate catalyzed by polymer supported Mg@PS-anthra complex.

Entry	Aldehydes	Ethylcyanoacetate	Time (h)	Product	Yield[a] (%)
1	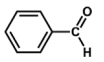		2	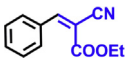	97
2	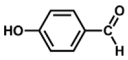		2	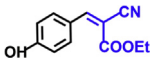	82
3	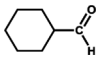		2	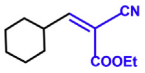	84
4	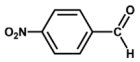		2	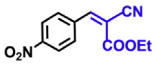	98
5	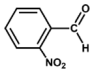		2	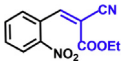	92
6	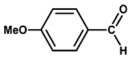		2	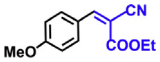	85
7	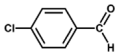		2	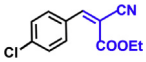	96
8	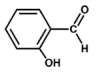		2	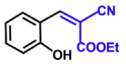	86
9			2	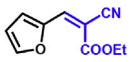	74
10			2	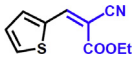	72

Reaction conditions: ethylcyanoacetate (2 mmol), aldehyde (1 mmol), catalyst (0.05 g), solvent-free, at room temperature.
[a] Yield was determined by GC.

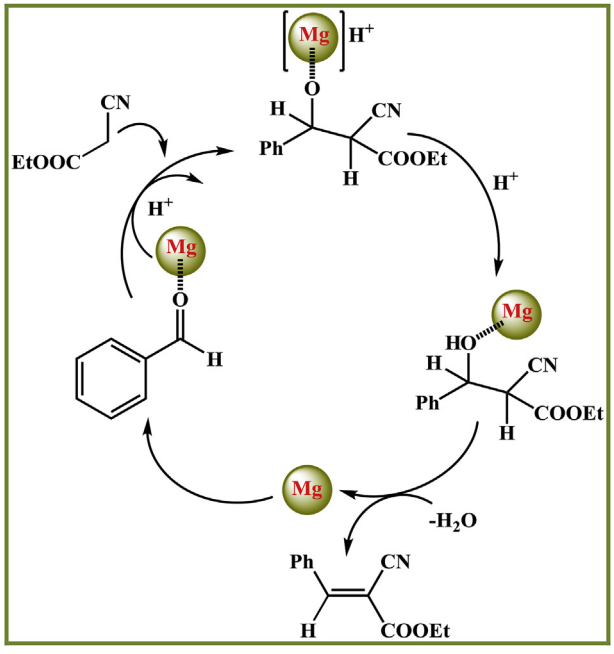

Scheme 5. Proposed reaction mechanism for the Knoevenagel condensation reaction.

centrifugation process. Then the isolated Mg@PS-anthra was thoroughly washed with water, acetone to get rid of all impurity if any and dried out in an air oven at 70 °C up to 6–7 h. With the separated catalyst the next successive runs were accomplished for both cyclo-addition of epoxide and Knoevenagel condensation reactions under the optimized condition. The Mg@PS-anthra complex can be efficiently recovered and recyclable up to five times without any significant decay in yields which clearly suggests that the Mg@PS-anthra complex is entirely heterogeneous in nature (Fig. 11). The prepared Mg@PS-anthra complex was successfully committed to the excellent recycling efficiency for both the synthesis of the cyclic carbonate and Knoevenagel condensation reaction.

In our recycling experiments, we have simultaneously studied the leaching of magnesium (if any) in our synthesized Mg@PS-anthra catalyst and the data are represented in Table 6. From this leaching limit study by AAS instrument we can conclude that after the first reaction cycle, no leaching of magnesium was observed. The AAS analysis recorded that after several reaction runs, a very negligible quantity of magnesium was leached out in our experiment compared to the other reported systems.

4. Conclusions

In summary, the polystyrene immobilized heterogeneous Mg catalyst (Mg@PS-anthra) has been synthesized. The catalyst was precisely characterized by powder XRD, SEM, IR, UV-vis, TGA and elemental analysis. An outstanding activity was achieved by the catalyst for the production of organic five-membered cyclic carbonates from epoxides in presence of CO_2 under atmospheric pressure at room temperature. It is shown that Mg@PS-anthra complex can also be used as a heterogeneous catalyst for Knoevenagel condensation reaction. The synthesized Mg@PS-anthra

Table 5
Comparison of catalytic activity of the Mg@PS-anthra catalyst in the cyclic carbonate reaction and Knoevenagel condensation with other reported systems.

Reaction	Catalyst	Reaction conditions	Yield (%)	[Ref.]
Cyclic carbonates	TiZiF	Styrene oxide (10 mol), CO_2 (25 psi), catalyst (1.0 mol%), 100 °C, 8 h	98	[46]
	Aluminium complexes of a series of bis(pyrazol-1-yl)methane	Styrene oxide (1.66 mmol), 10 bar of CO_2, catalyst (42.1 mg), Bu_4NBr (26.7 mg,0.083 mmol), RT, 24 h	83	[47]
	MCM-41-IPr–CO_2	Styrene oxide (50 mmol), CO_2 (2.0 MPa/19.72 atm), catalyst (0.25 mmol), CH_2Cl_2, 120 °C, 48 h	87	[48]
	Mg@PS-anthra	**Styrene oxide (5 mmol), CO_2 (1 atm), catalyst (30 mg), TBAB (5 mol %), RT, 6 h**	**97**	**This work**
Knoevenagel condensation	LDH-OH (Mg_3Al)	Benzaldehyde (10 mmol), ethyl cyanoacetate (10 mmol), catalyst (150 mg), Water, 60 °C, 10 h	94	[49]
	LDH-diisopropylamide	Benzaldehyde (2 mmol), ethyl cyanoacetate (2 mmol), catalyst (50 mg), DMF, RT, 2 h	95	[50]
	Aminopropyl-functionalized SBA-15	Benzaldehyde (10 mmol), ethyl cyanoacetate (10 mmol), catalyst (150 mg), Cyclohexane, 82 °C, 1 h	>99	[51]
	Mg–Ga/Al-MMO	Benzaldehyde (50 mmol), ethyl cyanoacetate (50 mmol), catalyst (1 wt%), 60 °C, Solvent-free, 4 h	82	[52]
	Mg@PS-anthra	**Benzaldehyde (1 mmol), ethyl cyanoacetate (2 mmol), catalyst (0.05 g), solvent-free, RT, 2 h**	**97**	**This work**

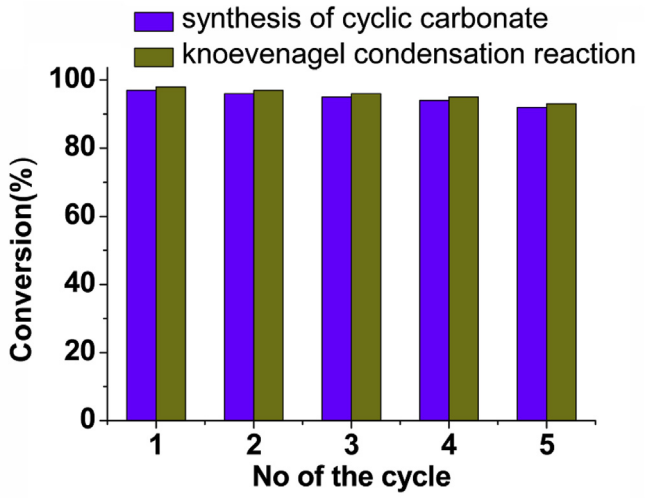

Fig. 11. Recyclability chart of Mg@PS-anthra complex catalyst under the optimized reaction conditions.

Table 6
Leaching limit of the Mg@PS-anthra catalyst in recycling experiments for both the cyclo addition of oxiranes and Knoevenagel condensation reactions.

Serial No.	Catalyst name	Reaction cycle	Leaching of Magnesium (ppm)	
			Cyclo addition of oxiranes	Knoevenagel condensation
1.	Mg@PS-anthra	1	0.00	0.00
2.	catalyst	2	0.004	0.002
3.		3	0.009	0.006
4.		4	0.016	0.009
5.		5	0.026	0.015

complex was evidenced as a very operative for the Knoevenagel condensation reaction using a variety of aldehydes with electron repelling and attracting groups providing high yields. The catalyst can be recovered and reused for five reaction cycles without any drop in its function and selectivity for both the reactions. These data nicely illustrate that the catalyst retains its stability under the optimized reaction conditions. The method described here is very simple and convenient to synthesize a series of cyclic carbonates and Knoevenagel condensation products under mild reaction conditions. Remarkably, all the reactions performed in presence of Mg@PS-anthra catalyst were found to undergo smoothly. The targeted products were obtained in satisfactory to excellent yields without the formation of unwanted products. In addition, it is expected that the current method offers many merits like cost-effectiveness, short reaction time and commercially important compounds without generation of any harmful waste at the end of the reaction.

Acknowledgements

S.M.I. acknowledges the Department of Science and Technology (DST-SERB, Project No. EMR/2016/004956), New Delhi, Govt. of India, and Board of Research in Nuclear Sciences (BRNS), Project reference No: 37(2)/14/03/2018-BRNS/37003, Govt. of India, for funding. AG expresses his sincere gratitude to the SERB-NPDF, DST, New Delhi, India (File No. PDF/2017/000478) for the National Post-Doctoral Fellowship. SMI is also thankful to Council of Scientific and Industrial and Research, CSIR (project reference no 02(0284)2016/EMR-II dated 06/12/2016) New Delhi, Govt. of India and Department of Science and Technology, West Bengal (DST-WB, Sanction No. 811(sanc.)/ST/P/S&T/4G-8/2014 Dated: 04.01.2016) for providing financial support. SMI acknowledges University of Kalyani, India for providing personal research grant. We sincerely acknowledge the DST and UGC, New Delhi, Govt. of India, for providing grant under FIST, PURSE and SAP program to the Department of Chemistry, University of Kalyani.

Appendix A. Supplementary data

Supplementary data to this article can be found online at https://doi.org/10.1016/j.jorganchem.2018.11.026.

References

[1] C. Song, Catal. Today 115 (2006) 2–32.
[2] (a) M. Peters, B. Kchler, W. Kuckshinrichs, W. Leitner, P. Markewitz, T.E. Müller, Chem Sus Chem 4 (2011) 1216–1240;
(b) M. Aresta, A. Dibenedetto, A. Angelini, Chem. Rev. 114 (2014) 1709–1742;
(c) A. Barthel, Y. Saih, M. Gimenez, J.D.A. Pelletier, F.E. Kühn, V. D'Elia, J.-M. Basset, Green Chem. 18 (2016) 3116–3123;
(d) R.M. Cuéllar-Franca, A. Azapagic, J. CO_2 Util. 9 (2015), 82–10;
(e) R. Khatun, P. Bhanja, P. Mondal, A. Bhaumik, D. Das, S.M. Islam, New J. Chem. 41 (2017) 12937–12946.
[3] (a) T. Sakakura, J.C. Choi, H. Yasuda, Chem. Rev. 107 (2007) 2365–2387;
(b) Z. Li, X. Ma, S. Xiong, Y. Ye, Z. Yao, Q. Lin, Z. Zhang, S. Xiang, New J. Chem. 42 (2018) 4495–4500;
(c) S. Wanga, R.J. Farrautoa, S. Karp, J.H. Jeon, E.T. Schrunk, J. CO_2 Util. 27 (2018)

390–397;
(d) V. D'Elia, J.D.A. Pelletier, J.-M. Basset, ChemCatChem 7 (2015) 1906–1917;
(e) S. Das, P. Mondal, S. Ghosh, B. Satpati, S. Deka, S.M. Islam, T. Bala, New J. Chem. 42 (2018) 7314–7325.
[4] (a) M. Cokoja, C. Bruckmeier, B. Rieger, W.A. Herrmann, F.E. Kühn, Angew. Chem. Int. Ed. 50 (2011) 8510–8537;
(b) R.A. Molla, K. Ghosh, B. Banerjee, M.A. Iqubal, S.K. Kundu, S.M. Islam, A. Bhaumik, J. Colloid Interface Sci. 477 (2016) 220–229;
(c) R.A. Molla, P. Bhanja, K. Ghosh, S.S. Islam, A. Bhaumik, S.M. Islam, ChemCatChem 9 (2017) 1939–1946;
(d) S. Ghosh, P. Bhanja, N. Salam, R. Khatun, A. Bhaumik, S.M. Islam, Catal. Today 309 (2018) 253–262;
(e) R.A. Molla, M.A. Iqubal, K. Ghosh, S.M. Islam, Green Chem. 18 (2016) 4649–4656;
(f) S.S. Islam, P. Bhanja, K. Ghosh, R.A. Molla, N. Yasmin D. Das, S.M. Islam, ChemistrySelect 2 (2017) 10595–10602.
[5] (a) D.J. Darensbourg, M.W. Holtcamp, Coord. Chem. Rev. 153 (1996) 155–174;
(b) A. Decortes, A.M. Castilla, A.W. Kleij, Angew. Chem. Int. Ed. 49 (2010) 9822–9837;
c) M. North, R. Pasquale, C. Young, Green Chem. 12 (2010) 1514–1539;
(d) B.H. Xu, J.Q. Wang, J. Sun, Y. Huang, J.P. Zhang, X.P. Zhang, S.J. Zhang, Green Chem. 17 (2015) 108–122;
(e) M. Cokoja, M.E. Wilhelm, M.H. Anthofer, W.A. Herrmann, F.E. Kühn, Chem Sus Chem 8 (2015) 2436–2454;
(f) S. Bhunia, R.A. Molla, V. Kumari, S.M. Islam, A. Bhaumik, Chem. Commun. 51 (2015) 15732–15735.
[6] M. Ree, J.Y. Bae, J.H. Jung, T.J. Shin, J. Polym. Sci. Polym. Chem. 37 (1999) 1863–1876.
[7] (a) K. Yagamuchi, K. Ebitani, H. Yoshida, K. Kaneda, J. Am. Chem. Soc. 121 (1999) 4526–4527;
(b) B.M. Bhanage, S. Fujita, Y. Ikushima, M. Arai, Appl. Catal. A Gen. 219 (2001) 259–266;
(c) H. Yasuda, L.N. He, T. Sakakura, J. Catal. 209 (2002) 547–550;
(d) S. Roy, B. Banerjee, A. Bhaumik, S.M. Islam, RSC Adv. 6 (2016) 31153–31160.
[8] L. Han, S.W. Park, D.W. Park, Energy Environ. Sci. 2 (2009) 1286–1292.
[9] W. Kuran, T. Loston, Macromol. Chem. Phys. 195 (1994) 977–980.
[10] (a) H. Büttner, L. Longwitz, J. Steinbauer, C. Wulf, T. Werner, Top. Curr. Chem. (2017), https://doi.org/10.1007/s41061-017-0136-5;
(b) S. Sopeña, E. Martin, E.C. Escudero-Adán, A.W. Kleij, ACS Catal. 7 (2017) 3532–3539;
(c) D. Ji, X. Lu, R. He, Appl. Catal. A Gen. 203 (2000) 329–333;
(d) H.S. Kim, J.J. Kim, B.G. Lee, O.S. Jung, H.G. Jang, S.O. Kang, Angew Chem. Int. Ed. Engl. 39 (2000) 4096–4098;
(e) R.L. Paddok, S.T. Nguyen, J. Am. Chem. Soc. 123 (2001) 11498–11499;
(f) X.B. Lu, R. He, C.X. Bai, J. Mol. Catal. A Chem. 186 (2002) 1–11;
(g) Y.M. Shen, W.L. Duan, J. Shi, J. Org. Chem. 68 (2003) 1559–1562;
(h) M. Ikiz, E. Ispir, E. Aytar, M. Ulusoy, S. Karabuga, M. Aslantas, O. Celik, New J. Chem. 39 (2015) 7786–7796.
[11] (a) M. Alves, B. Grignard, R. Mereau, C. Jerome, T. Tassaing, C. Detrembleur, Catal. Sci. Technol. 7 (2017) 2651–2684;
(b) H. Büttner, J. Steinbauer, C. Wulf, M. Dindaroglu, H.G. Schmalz, T. Werner, ChemSusChem 10 (2017) 1076–1079;
(c) J. Rintjema, A.W. Kleij, ChemSusChem 10 (2017) 1274–1282.
[12] (a) T. Aida, S. Inou, Macromolecules 15 (1982) 682–684;
(b) J.A. Martens, A. Bogaerts, N.D. Kimpe, P.A. Jacobs, G.B. Marin, K. Rabaey, M. Saeys, S. Verhelst, ChemSusChem 10 (2017) 1039–1055;
(c) F. d. l. C. Martínez, J. Martínez, M.A. Gaona, J.F. Baeza, L.F.S. Barba, A.M. Rodríguez, J.A. C-Osma, A. Otero, A.L. Sánchez, ACS Sustain. Chem. Eng. 6 (2018) 5322–5332.
[13] (a) J.A.C. Osma, J. Martínez, F. d. l. C. Martínez, M.P. Caballero, J.F. Baeza, J.R. López, A. Otero, A.L. Sánchez, J. Tejeda, Catal. Sci. Technol. 8 (2018) 1981–1987;
(b) L.L. Song, C. Chen, X.B. Chen, N. Zhang, New J. Chem. 40 (2016) 2904–2909.
[14] (a) S. Kumar, K. Prasad, J.M. Gil, A.J.F.N. Sobral, J. Koh, Carbohydr. Polym. 198 (2018) 401–406;
(b) D. Liu, G. Li, J. Liu, Y. Wei, H. Guo, ACS Appl. Mater. Interfaces 10 (2018) 22119–22129;
(c) M. Tu, R.J. Davic, J. Catal. 199 (2001) 85–91.
[15] R. Srivastava, D. Srinivas, P. Ratnasamy, Catal. Lett. 91 (2003) 133–139.
[16] (a) S. Biswas, R. Khatun, M. Sengupta, S.M. Islam, Mol. Catal. 452 (2018) 129–137;
(b) D.J. Darensbourg, Chem. Rev. 107 (2007) 2388–2410;
(c) J. Whiteoak, N. Kielland, V. Laserna, E.C. Escudero Adan, E. Martin, A.W. Kleij, J. Am. Chem. Soc. 135 (2013) 1228–1231;
(d) J. Ma, J.L. Song, H.Z. Liu, Z.F. Zhang, T. Jiang, H.L. Fan, B.X. Han, Green Chem. 14 (2012) 1743–1748;
(e) P. Pescarmona, M. Taherimehr, Catal. Sci. Technol. 2 (2012) 2169–2187.
[17] R. Khatun, P. Bhanja, R.A. Molla, S. Ghosh, A. Bhaumik, S.M. Islam, Mol. Catal. 434 (2017) 25–31.
[18] (a) S.A.E. Ayoubi, F.T. Boullet, J. Hamelin, Synthesis, 1994, pp. 258–260;
(b) I.G. Binev, Y.G. Binev, B.A. Stamboliyska, I.N. Juchnovski, J. Mol. Struct. 435 (1997) 235–239;
(c) G. Brufola, F. Fringuelli, O. Piermatti, F. Pizzo, Heterocycles 45 (1997) 1715–1721;
(d) B. Roy, A.S. Roy, A.B. Panda, S.M. Islam, A.P. Chattopadhyay, ChemistrySelect 1 (2016) 4778–4784;
(e) S.M. Islam, A.S. Roy, R.C. Dey, S. Paul, J. Mol. Catal. A Chem. 394 (2014) 66–73.
[19] (a) J.R. Harjani, S.J. Nara, M.M. Salunkhe, Tetrahedron Lett. 43 (2002) 1127–1130;
(b) F.A. Khan, J. Dash, R. Satapathy, S.K. Upadhyaya, Tetrahedron Lett. 45 (2004) 3055–3058.
[20] D. Prajapati, K.C. Lekhok, J.S. Sandhu, A.C. Ghosh, J. Chem. Soc. 1 (1996) 959–960.
[21] D.S. Bose, A.V. Narsaiah, J. Chem. Res. (2001) 36–38.
[22] T.I. Reddy, R.S. Verma, Tetrahedron Lett. 38 (1997) 1721–1724.
[23] (a) C.J. Li, T.H. Chan, Organic Reactions in Aqueous Media, John Wiley and Sons, New York, 1997, pp. 1–189;
(b) U.M. Lindstrom, Chem. Rev. 102 (2002) 2751–2772;
(c) P. Mondal, P. Bhanja, R. Khatun, A. Bhaumik, D. Das, S.M. Islam, J. Colloid Interface Sci. 508 (2017) 378–386;
(d) P. Basu, P. Bhanja, N. Salam, T.K. Dey, A. Bhaumik, D. Das, S.M. Islam, Mol. Catal. 439 (2017) 31–40 (e).
[24] D. Elhamifar, S. Kazempoor, J. Mol. Catal. A Chem. 415 (2016) 74–81.
[25] (a) J. Weitkamp, M. Hunger, U. Rymsa, Microporous Mesoporous Mater. 48 (2001) 255–270;
(b) P. Mondal, S. Ghosh, S.K. Das, A. Bhaumik, D. Das, S.M. Islam, Appl. Organomet. Chem. (2018), https://doi.org/10.1002/aoc.4227;
(c) P. Basu, S. Riyajuddin, T.K. Dey, A. Ghosh, K. Ghosh, S.M. Islam, J. Organomet. Chem. 877 (2018) 37–50;
(d) R. Khatun, S. Biswas, S. Ghosh, S.M. Islam, J. Organomet. Chem. 858 (2018) 37–46;
(e) T.K. Dey, K. Ghosh, P. Basu, R. Ali Moll, S.M. Islam, New J. Chem. 42 (2018) 9168–9176;
(f) P. Basu, T.K. Dey, A. Ghosh, S.M. Islam, J. Inorg. Organomet. Polym. Mater. 28 (2018) 1158–1170.
[26] J.I. Yu, S.Y. Shiau, A.N. Ko, Catal. Lett. 77 (2001) 165–169.
[27] S. Jaenicke, G.K. Chuah, X.H. Lin, X.C. Hu, Microporous Mesoporous Mater. 35–36 (2000) 143–153.
[28] J.O. Barth, A. Jentys, J. Kornatowski, J.A. Lercher, Chem. Mater. 16 (2004) 724–730.
[29] Q.C. Li, S.E. Brown, L.J. Broadbelt, J.G. Zheng, N.Q. Wu, Microporous Mesoporous Mater. 59 (2003) 105–111.
[30] Y.L. Wei, Y. Cao, J.H. Zhu, X.W. Yan, Chin. J. Inorg. Chem. 19 (2003) 233–239.
[31] S. Zhao, Y. Chen, Y.F. Song, Appl. Catal., A 475 (2014) 140–146.
[32] C.I. Ezugwu, B. Mousavi, M.A. Asraf, Z.X. Luo, F. Verpoort, J. Catal. 344 (2016) 445–454.
[33] S.M. Islam, A.S. Roy, P. Mondal, N. Salam, J. Mol. Catal. A Chem. 358 (2012) 38–48.
[34] S.M. Islam, A.S. Roy, P. Mondal, K. Tuhina, M. Mobarak, J. Mondal, Tetrahedron Lett. 53 (2012) 127–131.
[35] M.J. Kelly, A. Barthel, C. Maheu, O. Sodpiban, F. Dega, S.V.C. Vummaleti, E. Abou- Hamad, J.D.A. Pelletier, L. Cavallo, V. D'Elia, J. Basset, J. CO_2 Util. 20 (2017) 243–252.
[36] S.K.C. Soh, S.A. Jusoh, M.S.M. Yusof, W.M. Khairul, J. Sci. Res. Develop. 3 (4) (2016) 24–30.
[37] S. Sarkar, K. Dey, Spectrochim. Acta A 62 (2005) 383–393.
[38] G.G. Mohamed, M.M. Omar, A.H.H. Hindy, Spectrochim. Acta. A 62 (2005) 1140–1150.
[39] S.N. Riduan, Y. Zhang, Dalton Trans. 39 (2010) 3347–3357.
[40] (a) Y. Wang, J. Yao, H. Li, D.S. Su, M. Antonietti, J. Am. Chem. Soc. 133 (2011) 2362–2365;
(b) A.H. Chowdhury, P. Bhanja, N. Salam, A. Bhaumik, S.M. Islam, Mol. Catal. 450 (2018) 46–54.
[41] T.T. Wang, Y. Xie, W.Q. Deng, J. Phys. Chem. A 118 (2014) 9239–9243.
[42] M. North, R. Pasquale, Angew. Chem. Int. Ed. 48 (2009) 2946–2948.
[43] M.D. Gracia, M.J. Jurado, R. Luque, J.M. Campelo, D. Luna, J.M. Marinas, A.A. Romero, Microporous Mesoporous Mater. 118 (2009) 87–92.
[44] Y. Kubota, Y. Nishizaki, H. Ikeya, M. Saeki, T. Hida, S. Kawazu, M. Yoshida, H. Fujii, Y. Sugi, Microporous Mesoporous Mater. 70 (2004) 135–149.
[45] P. Pippal, P.P. Singh, Orient. J. Chem. 33 (4) (2017) 1736–1743.
[46] S. Verma, R.B.N. Baig, M.N. Nadagouda, R.S. Varma, Green Chem. 18 (2016) 4855–4858.
[47] J. Castro-Osma, A. Lara-Sánchez, M. North, A. Otero, P. Villuendas, Catal. Sci. Technol. 2 (2012) 1021–1026.
[48] H. Zhou, Y.M. Wang, W.Z. Zhang, J.P. Qu, X.B. Lu, Green Chem. 13 (2011) 644–650.
[49] K. Ebitani, K. Motokura, K. Mori, T. Mizugaki, K. Kaneda, J. Org. Chem. 71 (2006) 5440–5447.
[50] M.L. Kantam, A. Ravindra, C.V. Reddy, B. Sreedhar, B.M. Choudary, Adv. Synth. Catal. 348 (2006) 569–578.
[51] X.G. Wang, K.S.K. Lin, J.C.C. Chan, S. Cheng, J. Phys. Chem. B 109 (2005) 1763–1769.
[52] I. Rousselot, C.T. Guého, J.P. Besse, Int. J. Inorg. Mater. 1 (1999) 165–174.